EBR-II SHRT-17 and SHRT-45R Benchmark Analyses

T. Sumner, A. Moisseytsev, T.Y.C. Wei, T. Fei

Argonne National Laboratory, Argonne, IL, USA

E-mail contact of main author: tsumner@anl.gov

Abstract. In 2012, the International Atomic Energy Agency established a coordinated research project on the EBR-II Shutdown Heat Removal Tests SHRT-17 and SHRT-45R. These two tests were the most severe protected and unprotected loss of flow tests performed during the SHRT program. Nineteen organizations representing eleven countries participated in the benchmark. Argonne simulated the SHRT-17 and SHRT-45R tests using the sodium fast reactor safety analysis code SAS4A/SASSYS-1, with neutronics analyses performed using the Argonne fast reactor neutronics analysis tools suite. Argonne's simulations during phase 1, which were performed before the experimental data was provided to all participants, produced reasonable agreement with the measured data for SHRT-45R. But for SHRT-17, overpredicted flow rates after the beginning of the test led to underpredicted temperatures. This discrepancy was corrected during phase 2 by properly accounting for the resistance of the locked pumps and the circumstances under which the pumps were assumed to lock. Additional analyses were performed for SHRT-45R with the reference power level used as a boundary condition to assess the performance of the systems model, allowing for more accurate analysis of the primary system model without power discrepancies affecting predicted flow rates and temperatures. The results of these benchmark simulations demonstrate that SAS4A/SASSYS-1 successfully captures EBR-II's response to these two severe accidents.

Key Words: EBR-II, SAS4A/SASSYS-1, SHRT-17, SHRT-45R.

1. Introduction

In 2012, the International Atomic Energy Agency (IAEA) established a coordinated research project (CRP) on EBR-II Shutdown Heat Removal Tests (SHRT). [1] The objectives of the CRP, which concluded in 2016, [2] were to improve design and simulation capabilities in fast reactor neutronics, thermal hydraulics, plant dynamics, and safety analyses through benchmark analysis of two landmark tests performed during the EBR-II SHRT program. The selected tests were SHRT-17 and SHRT-45R, the most severe protected and unprotected loss of flow tests performed during the SHRT program, respectively.

The benchmark was performed in two phases. During the first phase, [3] participants had no access to the recorded data from either test. Once all phase 1 calculations were completed in February 2014, phase 2 was initiated with participants receiving experimental data. [4]

In addition to its role as the lead technical organization for the CRP, Argonne also performed analyses as a participant in the CRP. Argonne simulated the SHRT-17 and SHRT-45R tests using the sodium fast reactor safety analysis code SAS4A/SASSYS-1. [5] Neutronics analyses were performed with the Argonne fast reactor neutronics analysis tools suite. [6-9] Reasonable agreement with the experimental data was obtained for the initial simulation results for SHRT-45R, but flow rates were significantly overpredicted for SHRT-17. Modeling improvements made during phase 2 brought the simulation results and experimental data for both tests into better agreement.

2.   Simulation Model

2.1. Systems Model

Core models in SAS4A/SASSYS-1 consist of a number of single-pin channels and optional subchannels. A single-pin channel represents the average pin in a subassembly, and subassemblies with similar reactor physics and thermal-hydraulic characteristics can be grouped together. SAS4A/SASSYS-1 models include an axial zone to represent the fueled and gas plenum regions and up to six upper and lower reflector zones. Each axial zone is connected to a structure region, which can be used to model components such as the wire-wrap or duct walls.

Single-pin channel models were developed for the driver, partial driver, control, dummy, reflector, and blanket subassemblies. Each of the 637 subassemblies for the SHRT-17 and SHRT-45R core configurations was modeled with one of these six channel types. FIG. 1 illustrates the channel assignments for each of the subassemblies for the SHRT-45R test. This 22-channel model was used for most of the SAS4A/SASSYS-1 analyses. A similar model was created for the SHRT-17 core model. Additional analyses were performed where the XX09 and XX10 instrumented subassemblies, and their six neighboring subassemblies, were modeled using the SAS4A/SASSYS-1 subchannel model; however, those analyses are not discussed here.

The PRIMAR-4 module in SAS4A/SASSYS-1 simulates the thermal hydraulics of the heat transport systems outside the core. Compressible volumes, or CVs, are zero-dimensional volumes that are used to model larger volumes of coolant such as inlet and outlet plena and pools. Compressible volumes are connected by liquid segments, which are composed of one or more elements. Elements are modeled by one-dimensional, incompressible, single-phase flow and can be used to model pipes, valves, heat exchangers, steam generators, and more. FIG. 2 illustrates the EBR-II primary heat transport system model.
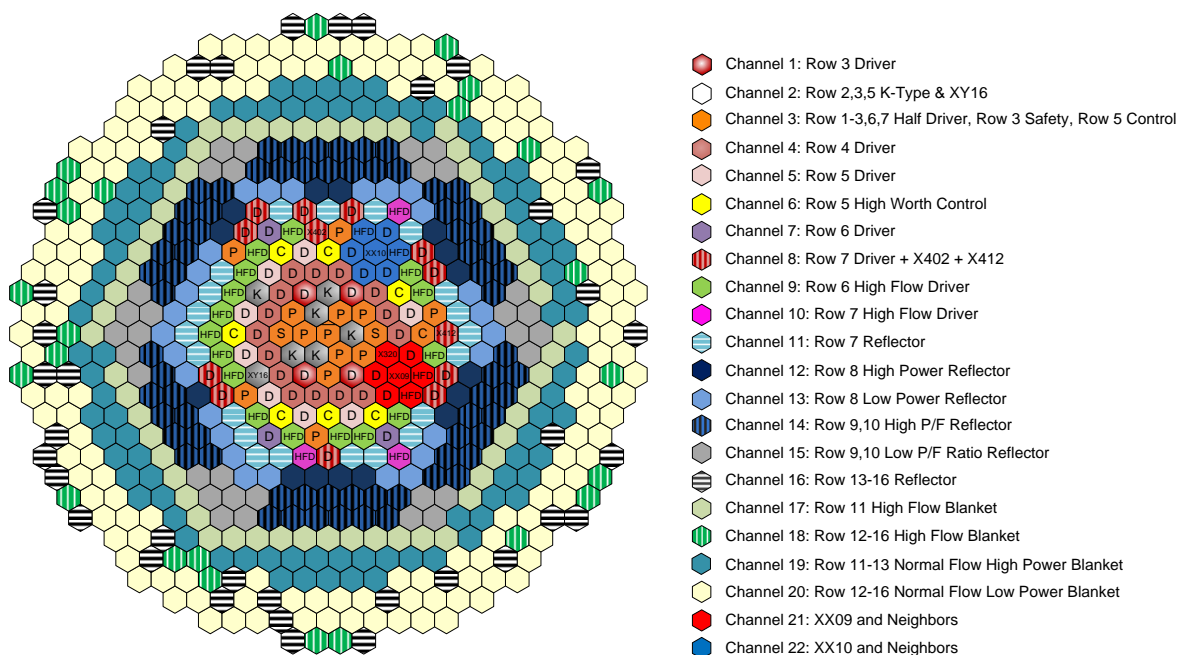

Channel 1: Row 3 Driver
Channel 2: Row 2,3,5 K-Type & XY16
Channel 3: Row 1-3,6,7 Half Driver, Row 3 Safety, Row 5 Control
Channel 4: Row 4 Driver
Channel 5: Row 5 Driver
Channel 6: Row 5 High Worth Control
Channel 7: Row 6 Driver
Channel 8: Row 7 Driver + X402 + X412
Channel 9: Row 6 High Flow Driver
Channel 10: Row 7 High Flow Driver
Channel 11: Row 7 Reflector
Channel 12: Row 8 High Power Reflector
Channel 13: Row 8 Low Power Reflector
Channel 14: Row 9,10 High P/F Reflector
Channel 15: Row 9,10 Low P/F Ratio Reflector
Channel 16: Row 13-16 Reflector
Channel 17: Row 11 High Flow Blanket
Channel 18: Row 12-16 High Flow Blanket
Channel 19: Row 11-13 Normal Flow High Power Blanket
Channel 20: Row 12-16 Normal Flow Low Power Blanket
Channel 21: XX09 and Neighbors
Channel 22: XX10 and Neighbors
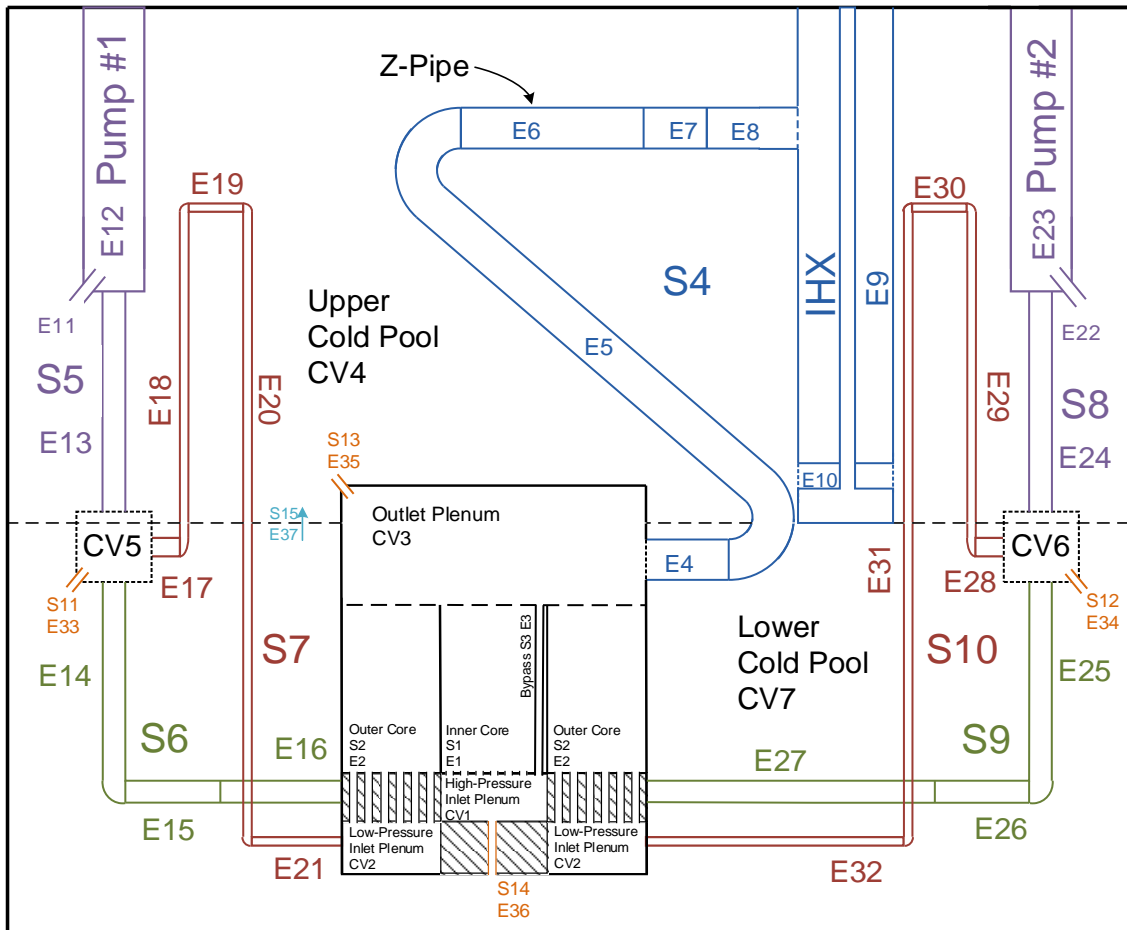
FIG. 1. SHRT-45R Core Channels

FIG. 2. Primary System Model Geometry

SAS4A/SASSYS-1 models employ a point kinetics model, which assumes a time-independent reactor power spatial profile, to calculate the reactor power level. This model was used to predict the power level for the unprotected SHRT-45R transient. Reactivity feedback coefficients and axial power profiles were generated using the Argonne fast reactor neutronics analysis tools suite.

2.2. Neutronics Model

MC^2-3/TWODANT was used to generate neutron and photon cross sections, the neutron flux to photon source conversion matrix, and neutron and photon KERMA factors. [6,7] Cross section generation was performed with a two-step MC^2-3 calculation. The first step used a 1041-group neutron cross section library and performed a 2-dimensional RZ transport calculation using TWODANT to calculate the neutron flux spectrum for various regions in the core. In the second step, the flux spectrum obtained from the first step was used to condense the neutron library to 33 groups.

Using the 33 group results from TWODANT, a hexagonal-Z DIF3D model was employed with both diffusion and P3 angular approximation to evaluate the power distribution in the EBR-II core. [8] DIF3D was also used to evaluate the axial and radial expansion reactivity feedback coefficients and the control and safety subassembly worth curve. The delayed neutron fraction, Doppler, fuel, clad, structure and sodium void reactivity feedback coefficients were evaluated with PERSENT and VARI3D. [9]

3.   Initial Results

3.1. SHRT-17

Although Argonne's SHRT-17 simulation during the blind phase of the CRP predicted similar trends as the measured test data, overpredicted flow rates after the beginning of the test led to underpredicted temperatures. The left side of FIG. 3 compares Argonne's predicted flow rates with the flow rates measured in the high- and low-pressure piping following primary pump #2. Measured flow rates for pump #1 were unavailable for the SHRT tests. The predicted low-pressure flow rate agreed well with the measured data throughout the transient. During the first minute of the test while the pump speed was still coasting down, the high-pressure flow rate was well predicted. However, issues that were later identified with the pump input parameters led to over-predicted pump #2 high-pressure flow rates.

Because the high-pressure flow rate represented approximately 85% of the total core flow rate, discrepancies for the high-pressure flow rate had a larger effect on the rest of the simulation than discrepancies for the low-pressure flow rate. Accurate predictions of upper plenum, Z-Pipe, and IHX temperatures require accurate core flow rate predictions. For the initial SHRT-17 simulations, Argonne's model predicted correctly the core outlet temperature during the beginning of the test. But as the test continued and the high-pressure flow was overpredicted, the core outlet temperature was underpredicted by 20-30 degrees. The right side of FIG. 3 illustrates the predicted and measured core outlet temperature.
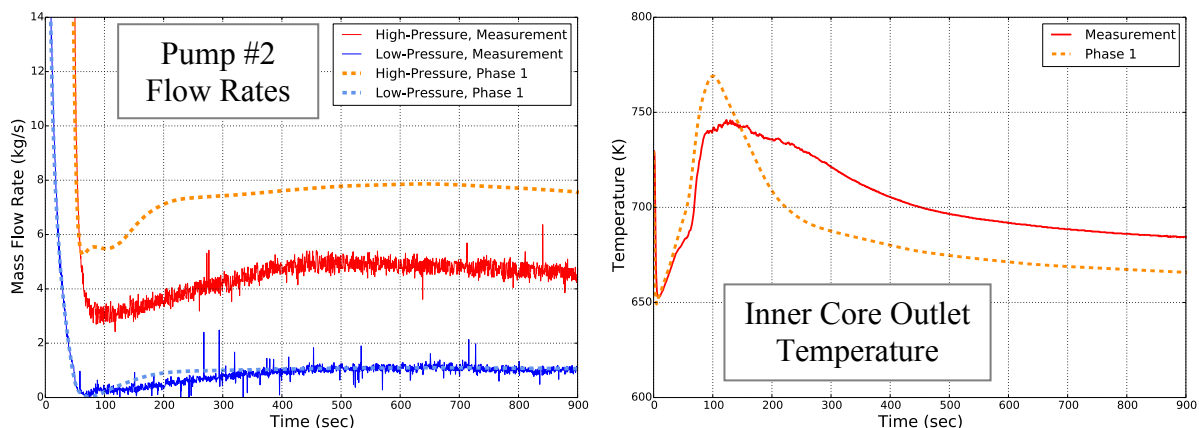

FIG. 3. SHRT-17 Initial Results

3.2. SHRT-45R

Initial predictions of the SHRT-45R flow rates through the core inlet piping, which are illustrated by the left side of FIG. 4, agreed much better with the measured data for SHRT-45R than for SHRT-17. The flow rate predictions were most accurate during the initial flow coastdown and the second half of the transient. During the middle part of the transient, the model predicts a slightly lower flow rate when the pump coastdown ends. Accurate predictions of the high-pressure flow rate are necessary for reactivity feedback calculations and accurate predictions of the power level during the transient.

The low-pressure flow rate was overpredicted by approximately 50%, but this flow rate represents only 15% of the total core flow rate. Because the low-pressure piping feeds the reflector and blanket subassemblies, discrepancies in the flow rates for those subassemblies do not significantly affect the core power level during the transient.
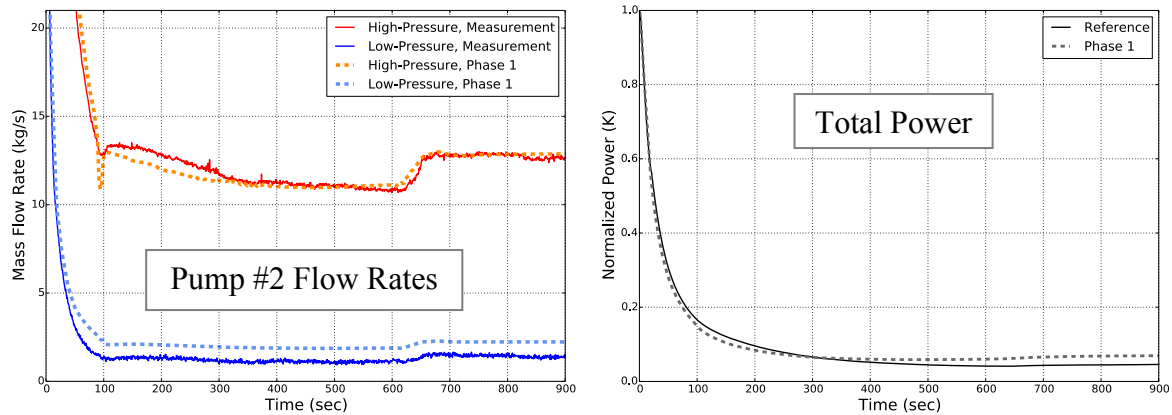
FIG. 4. SHRT-45R Initial Results

Total power was predicted reasonably well for SHRT-45R, as shown by the right side of FIG. 4. Agreement was better during the first half of the test. During the second half of the test, the power level was very low, around 5%, so small absolute differences led to larger relative differences. This discrepancy during the second half of the test led to the Z-Pipe inlet temperature being overpredicted later in the test.

The predicted Z-Pipe inlet temperature agreed well with the measured data for the first half of the transient. The measured Z-Pipe inlet temperature rose more slowly than the predicted temperature, but this is to be expected because the upper plenum was modeled with a zero-dimensional volume. Thermal stratification and delays as sodium flowed around a flow baffle plate in the upper plenum were not captured by the SAS4A/SASSYS-1 model.

4. Final Results

4.1. SHRT-17

After phase 1 concluded, Argonne's efforts focused on improving agreement between the measured data and predicted results. FIG. 5 illustrates Argonne's final SHRT-17 predictions. The largest improvement was made for the SHRT-17 flow rate predictions. While pump #1 locked during the initial SHRT-17 simulation, pump #2 did not lock. In contrast, both pumps locked for the SHRT-45R simulation. Locking occurs when the flow rate and pump speed are low enough that the rotor stops spinning and becomes a hydraulic resistance.

An evaluation of the measured flow rates and pump speeds for both tests suggested that the pumps should have locked for SHRT-17 but possibly not during the actual SHRT-45R test. It was therefore assumed that a calibration error produced an elevated measured speed for pump #2 during SHRT-17. The speed for the pump was decreased to zero after the flow coastdown to ensure that the pump locked.

During phase 1, a pump locked rotor loss coefficient of 1.0 was assumed, which produced reasonably good agreement for SHRT-45R. But too little resistance through the pumps likely caused the elevated SHRT-17 flow rate predictions. A parametric analysis of the loss coefficient found that a value of 3.6 was necessary for accurate SHRT-17 flow rate predictions. These adjustments led to a more accurate high-pressure flow rate prediction for SHRT-17 but affected the SHRT-45R predictions as discussed in the next section.

The low-pressure inlet plenum temperature decreased several degrees, likely due to heating and cooling in the upper and lower parts of the stratified cold pool. The model did not capture the heat transfer between sodium in the inlet pipes and the stratified cold pool. This effect does not significantly affect the simulation results. Large thermal inertia in the cold pool led to flat predictions for the core inlet temperatures.

Because the flow rates were no longer overpredicted, the core outlet temperature agreed much better with the test measurement. Multiple thermocouple measurements were combined to produce the measured core outlet temperature shown in FIG. 5, but the specific thermocouples could not be identified. However, the measurement is similar to many of the individual inner core subassembly outlet temperature measurements. Therefore, this measurement is compared against the predicted inner core outlet temperature, which agrees reasonably well.

The most difficult measurement to predict for either test was the IHX primary side inlet temperature. The inlet thermocouple was located behind multiple impact baffle plates and near one of the IHX tubes. Based on steady-state measurements, the primary side rejected 53 MW to the intermediate sodium. The intermediate IHX temperature measurements, which are consistent with temperature measurement upstream and downstream of the IHX, produced a heat transfer rate of 60 MW, the same as the initial reactor power level. Additionally, losses through the primary vessel walls were too small to account for the 7 MW difference. Based on this evidence, it was concluded that the measured IHX inlet temperature did not represent the average temperature of sodium leaving the Z-Pipe and entering the IHX. Higher fidelity models would be required to capture the effects in the IHX inlet region. The discrepancy between the measured data and the SAS4A/SASSYS-1 predictions is considered acceptable.
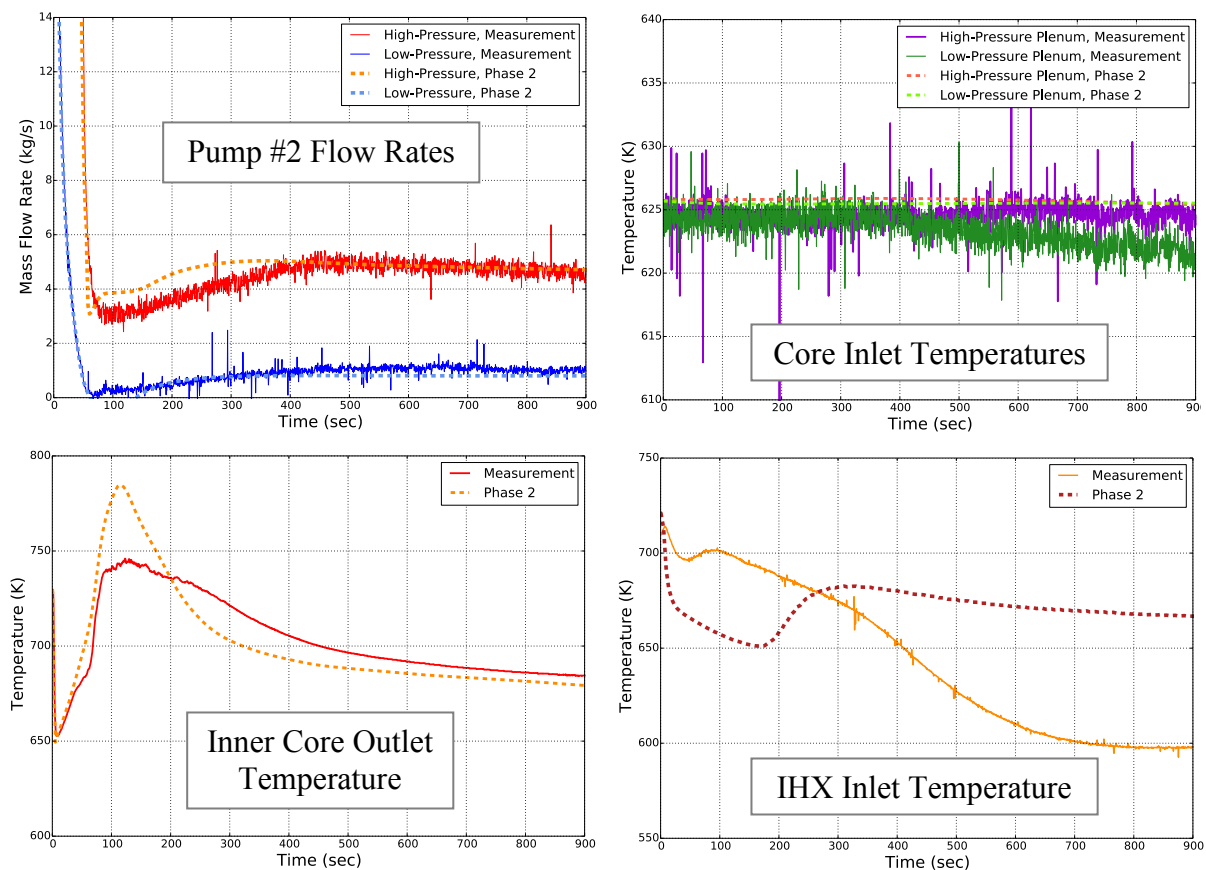

FIG. 5. SHRT-17 Final Results

4.2. SHRT-45R

In order to maintain model consistency for the two tests, modifications made to the pump model for SHRT-17 were also applied to the SHRT-45R model. The SHRT-17 analyses resulted in a higher pump locked rotor loss coefficient, which led to significantly underpredicted SHRT-45R flow rates. Because the transient SHRT-45R flow rates were nearly 2.5 times larger than for SHRT-17, it was speculated that natural circulation and the auxiliary EM pump head prevented the pump rotors from locking during SHRT-45R. Therefore, the pump locking thresholds were reduced to prevent locking during the SHRT-45R simulation. Overall, these changes resulted in significantly better flow rate agreement for SHRT-17 while the SHRT-45R flow rate increased only slightly and still agreed well with the measured data. FIG. 6 illustrates the final results for SHRT-45R.
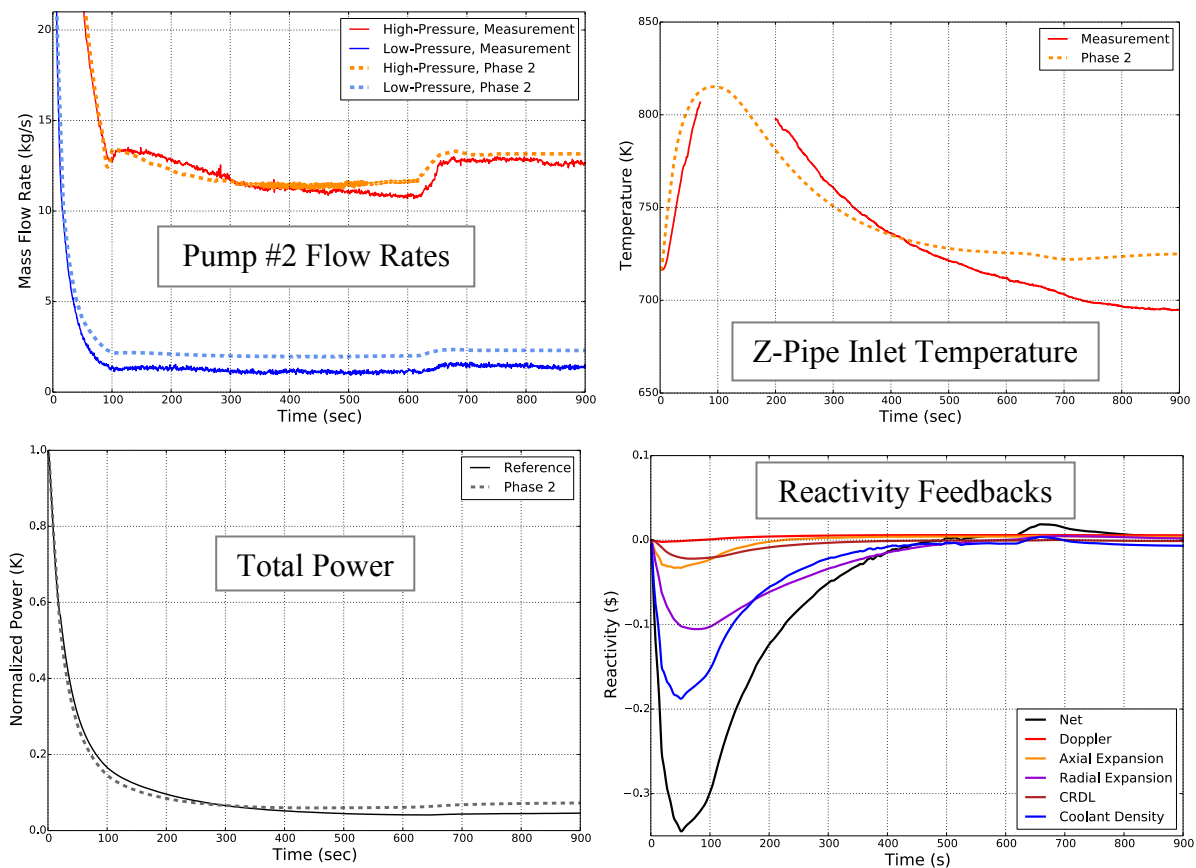

FIG. 6. SHRT-45R Final Results

Higher phase 2 flow rates led to lower core outlet temperatures and therefore lower temperatures in the Z-Pipe. The predicted Z-Pipe inlet temperature rose faster than the measured data because the upper plenum was modeled as a zero-dimensional volume. There was no delay as hotter sodium entered the volume, flowed through or around the upper plenum flow baffle plate, and entered the Z-Pipe. During the second half of the test, overpredicted power led to an overpredicted Z-Pipe inlet temperature.

FIG. 6 shows a comparison between the predicted SHRT-45R total power and the reference power, which is the sum of the measured fission power and calculated decay heat. Reactivity feedback coefficients were not updated after phase 1 so the initial and final reactivity feedback and power predictions are very similar. The predicted power is higher than the

reference power at the end of the test partly because of the higher predicted core flow rate, which produced lower in-core temperatures. While the absolute differences between the predicted and measured power levels were small, the relative differences cannot be neglected. Total power was underpredicted by nearly 20% during the first 200 seconds. At the end of the test, when total power was low, it was overpredicted by 60%.

Separate analyses were performed using test measurements at the core inlet as boundary conditions. Both the core inlet temperature and flow rate predictions agreed well with data measurements, but there were still small discrepancies. Using the measurements as boundary conditions reduced the power overprediction at the end of the test from 60% to 33%. Data uncertainties may account for some of the remaining discrepancy. After the pumps tripped, flow rates fell within a range at which the flowmeters were known to have larger uncertainties, especially the low-pressure flow rate. The simulation flow rate, therefore, may not match exactly the actual test flow rate so some discrepancy could remain. But this analysis demonstrates that further reduction of the flow rate and core inlet temperature discrepancies would improve the power predictions.

Next, sensitivity studies were performed to determine how sensitive the power prediction is to the reactivity feedback coefficients and what would be required to further reduce the 33% discrepancy. Only two of the reactivity feedback effects, sodium density and radial core expansion, were large enough to affect the power prediction significantly. However, unrealistically large changes in the feedback coefficients for those effects would be required to obtain significantly improved agreement with the reference power data. The SAS4A/SASSYS-1 model used a simple radial expansion model that does not account for subassembly bowing. SAS4A/SASSYS-1 includes a radial expansion reactivity feedback model for limited free bow type core restraint systems. But EBR-II employed a free standing core restraint system, which cannot be represented by the models in SAS4A/SASSYS-1. A model that can capture subassembly bowing, which may have resulted in inward bowing at elevated temperatures, would be needed to achieve even better agreement between the predicted and reference power data.

Analyses were also performed to evaluate the primary heat transport system model by enforcing the measured total power level during SHRT-45R. As shown in FIG. 7, the high-pressure flow rate and Z-Pipe inlet temperature predictions agree very well with the measured data when power is used as a boundary condition. By eliminating the power discrepancy, the effect of underpredicted or overpredicted temperatures is significantly reduced, demonstrating the accuracy of the EBR-II primary system model.
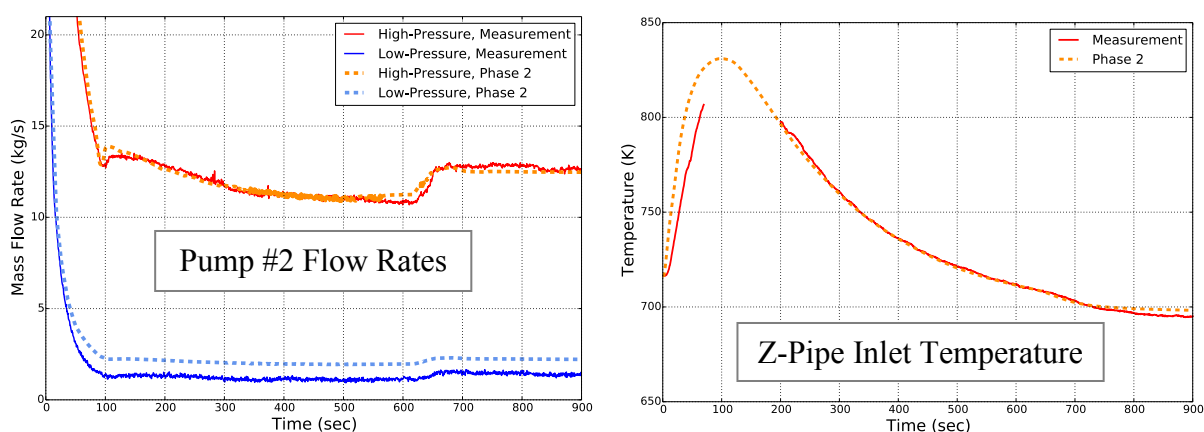

FIG. 7. SHRT-45R Results, with Power as a Boundary Condition

5. Neutronics Results

Results of the neutronics calculations are summarized in Table I. The table provides k_{eff}, β_{eff} and reactivity feedback coefficients calculated by DIF3D using finite difference diffusion theory and by VARIANT using P3 variational nodal theory. Agreement between the diffusion and transport results is in line with expectations. Because diffusion theory struggles with neutron leakage, it was expected to produce a lower k_{eff} for EBR-II's high leakage core.

The MCNP6 calculation was performed using the geometry from the DIF3D model. [10] The difference between the MCNP6 and VARIANT results is less than 200 pcm, which is within the expected range. Such close agreement suggests k_{eff} was not less than 1.0 because of the chosen computational methods. Discrepancies in the fuel compositions, which were calculated using fission gas compositions, and an inability to measure the actual subassembly pitch spacing are two sources of uncertainty that could have produced a lower value of k_{eff}. EBR-II's subassembly ducts had spacer buttons that were intended to maintain adequate spacing. But slippage of these buttons may have led to inward subassembly bowing.

TABLE I: NEUTRONICS PARAMETERS AND REACTIVITY FEEDBACK COEFFICIENTS

Parameters	Units	DIF3D FDD	VARIANT	MCNP6
k_{eff}	-	0.9670	0.9885	0.9904
βeff	pcm	705	705	-
Axial Expansion	pcm/K	-0.36	-0.65	-
Radial Expansion	pcm/K	-1.78	-1.67	-
Sodium Density	pcm/K	-1.70	-1.49	-
Doppler	pcm/K	-0.06	-0.06	-

6. Summary and Conclusions

Argonne used the fast reactor safety analysis code SAS4A/SASSYS-1 to perform simulations of the protected and unprotected loss of flow tests SHRT-17 and SHRT-45R. Reactivity feedback coefficients and other neutronics parameters were calculated using Argonne's fast reactor neutronics analysis tools suite. Initial predictions for phase 1 of the benchmark produced good agreement with the measured test data, but there was room for improvement.

In phase 2, adjustments to the model, in particular the thresholds for pump locking and the hydraulic resistance of a locked pump, led to good agreement with the measured data for both tests. The largest remaining discrepancies for both tests were with the measured pump #2 low-pressure flow rate, which dropped to a range with higher uncertainty, and the IHX inlet temperature, which was measured by a thermocouple that was strongly influenced by its location and therefore could not capture the average temperature of sodium entering the IHX. Predicting this measurement well would require higher fidelity models such as a coupled systems-CFD simulation.

Additional analyses were performed for SHRT-45R to assess the power prediction and primary system heat transport model independently. By eliminating any power discrepancies resulting from the point kinetics model, the heat transport system model was demonstrated to accurately predict the primary system flow rate and core outlet temperatures. Small

discrepancies in the core inlet temperature and flow rates accounted for half of the difference between the predicted and reference power data at the end of SHRT-45R. Sensitivity studies were also performed for the reactivity feedback coefficients, which led to the conclusion that further improvement to the power prediction would require a radial expansion model that accurately predicts subassembly bowing resulting from EBR-II's free standing core restraint system.

The results of these benchmark calculations demonstrate that SAS4A/SASSYS-1 successfully captures the response of EBR-II to these two severe accidents.

Acknowledgements

References

[1]   BRIGGS, L. L., *et. al.*, "EBR-II Passive Safety Demonstration Tests Benchmark Analyses", International Conference on Fast Reactors and Related Fuel Cycles: Next Generation Nuclear Systems for Sustainable Development (FR17), Yekaterinburg, Russian Federation, June 26-29, 2017. Manuscript submitted for publication.

[2]   INTERNATIONAL ATOMIC ENERGY AGENCY, Benchmark Analyses of EBR-II Shutdown Heat Removal Tests, IAEA-TECDOC, IAEA, Vienna (2017, under review

[3]   BRIGGS, L. L., T. SUMNER, T. FEI, T. SOFU, and S. MONTI, "EBR-II Passive Safety Demonstration Tests Benchmark Analyses – Phase 1", Trans. Amer. Nucl. Soc., Anaheim, California, USA, November 9-13, 2014, 111, pp. 1263-1266.

[4]   BRIGGS, L. L., *et al.*, "EBR-II Passive Safety Demonstration Tests Benchmark Analyses – Phase 2", *Proc. of the 16th International Topical Meeting on Nuclear Reactor Thermal Hydraulics (NURETH-16)*, Chicago, Illinois, USA, August 30-September 4, 2015.

[5]   FANNING, T.H., *et. al.*, "The SAS4A/SASSYS-1 Safety Analysis Code System", ANL/NE-12/4, Argonne, IL, January 31, 2012.

[6]   LEE, C. H. and W. S. YANG, "Development of Multigroup Cross Section Generation Code MC^2-3 for Fast Reactor Analysis", Proc. of Int. Conf. on Fast Reactors and Related Fuel Cycles (FR09), Kyoto, Japan, Dec. 7-11, 2009.

[7]   ALCOUFFE, R. E., F. W. BRINKLEY, D. R. MARR, and R. D. O'DELL, "User's Guide for TWODANT: A Code Package for Two-Dimensional, Diffusion-Accelerated Neutral Particle Transport," Los Alamos National Laboratory, LA-10049-M, 1984.

[8]   G. PALMIOTTI, B. CARRICO, E. E. LEWIS, "Variational nodal transport methods with anisotropic scattering," Nuclear Science and Engineering, Vol. 115, pp. 233-243 (1993).

[9]   SMITH, M. A., C. ADAMS, W. S. YANG, and E. E. LEWIS, "VARI3D & PERSENT: Perturbation and Sensitivity Analysis," ANL/NE-13/8, Argonne National Laboratory, 2013.

[10]   J.T. GOORLEY, et al., "Initial MCNP6 Release Overview - MCNP6 version 1.0," LA-UR-13-22934, Los Alamos National Laboratory (2013).